Article

Diagenetic Genesis and Evolution of Coal-Bearing Tight Sandstone Reservoir in the Yangxia Formation, Northern Kuqa Depression, Tarim Basin

Huajun Guo, Wenhao Xia,* Xiang Shan, Kelai Xi, Bo Peng, Xianzhang Yang, Zhiwen Zou, and Wenfang Yuan

Read Online

ACCESS | Metrics & More | Article Recommendations

ABSTRACT: Coal seams of the Yangxia Formation are widespread in the northern part of the Kuqa Depression in the Tarim Basin. During the thermal evolution of the coal seams, the generated fluids of different periods and natures have a significant impact on tight sandstone reservoirs. To further investigate the diagenetic characteristics and reservoir genesis of the tight sandstones due to the influence of coal seams, an in-depth exploration of the causes of dissolution and cementation in the reservoirs was conducted through thin-section casting, cathode luminescence, scanning electron microscopy, carbon−oxygen isotopic analyses, and X-ray diffraction of whole rock and authigenic clay minerals, along with burial evolution history and fluid evolution history. It is suggested that two phases of acidic fluids are mainly produced during the thermal evolution process of coal seams, including an early humic acid and a late organic carboxylic acid. The early phase humic acid plays a purifying role in reservoirs with coarse particles, rigidity-rich particles, and good permeability conditions. It selectively dissolves sedimentary calcareous mud and calcite, and the dissolution products are completely migrated. At the same time, it inhibits early carbonate cementation. The late organic carboxylic acid will dissolve potassium feldspar and some volcanic rock debris, and the dissolution products are difficult to migrate under the sealing conditions caused by lithological differences, which often take the cementation form of siliceous overgrowth and kaolinite or illite. In addition to the cementation resulting from the dissolution products of acidic fluids produced by the coal seams, the CO_2-rich fluids generated by the coal seam thermal evolution will combine with ions such as Ca^{2+} from different sources, resulting in two phases of carbonate cementation. Based on the above research, this study summarizes a set of diagenetic evolution models for coal-bearing reservoirs.

1. INTRODUCTION

Currently, conventional oil and gas resources are gradually becoming unable to meet the current industrial development needs at global production rates. In order to solve the energy shortage, petroleum geologists are focusing on available larger reserves of unconventional oil and gas resources. As an important part of unconventional oil and gas resources, tight sandstone reservoirs play an irreplaceable role.[1−5] At present, tight oil and gas in the United States, Canada, Russia, and other countries are developing rapidly.[3,4] China's tight oil and gas resources are also very rich, mainly distributed in the Tarim Basin, Ordos Basin, Junggar Basin, Songliao Basin, Sichuan Basin, Bohai Bay Basin, Qaidam Basin, and other Mesozoic and Cenozoic oil-bearing basins.[3,6−9] The reservoirs in these basins are mainly characterized by tight sandstones that are distributed over large areas and associated with, or in contact with, source rocks.[6] Among these, the Tarim Basin is the largest oil-bearing basin in China, and its oil−gas resources are

very rich.[3,4,9] In 2021, the equivalent oil and gas production in the Tarim Basin will exceed 30 million tons, including 6.042 million tons of oil and 30.07 billion cubic meters of natural gas. The Kuqa Depression in the north of the Tarim Basin is an important oil- and gas-producing area.[10]
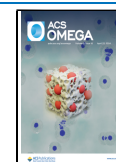
Several sets of continental source rocks are developed in the Kuqa Depression, and the Triassic−Jurassic coal seam is the source rock for most of the natural gas and for a small part of the oil in this area.[11−13] The Yangxia Formation is widely distributed in the northern part of the Kuqa Depression with
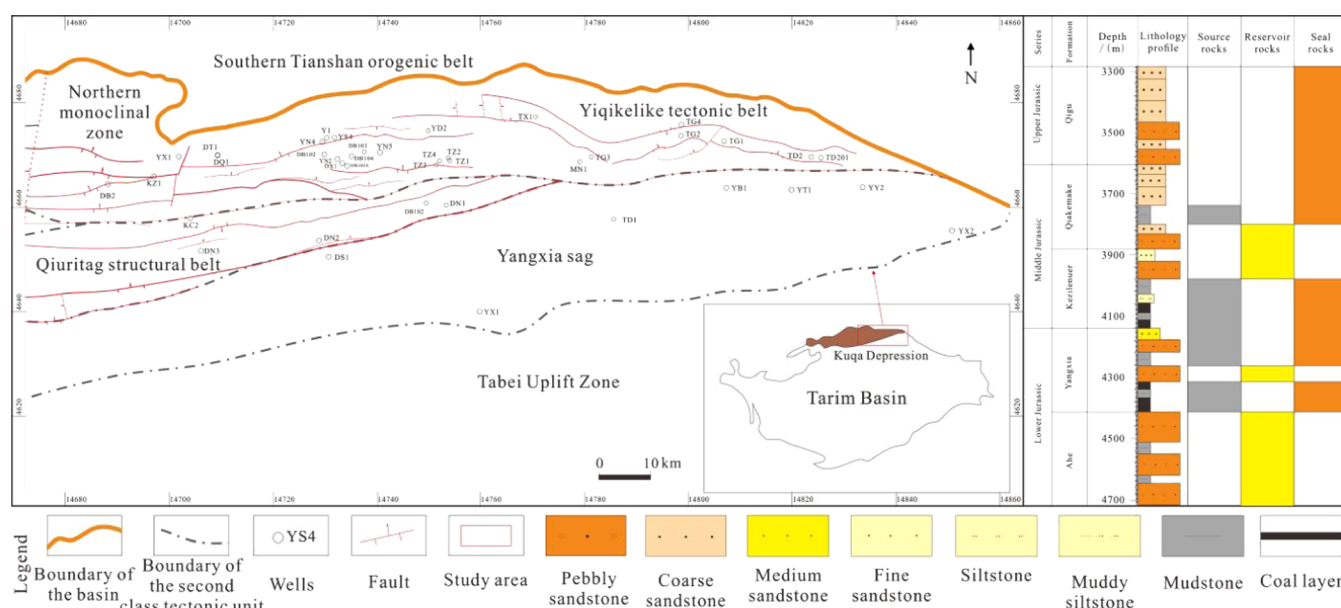
Figure 1. Tectonic location map and sedimentary facies of the Yangxia Formation in the study area.[9,28] [Reprinted in part with permission from ref 9. Copyright (2021) (Acta Petrolei Sinica); and reprinted in part with permission from ref 28. Copyright (2018) (China National Knowledge Infrastructure)].

developed sedimentary facies, such as lakes, swamps, and braided river deltas. It is under the control of these sedimentary facies within the formation that massive mudstone and coal seams have been formed. The maturity values of source rocks in the Yangxia Formation are mostly between 0.5 and 1.08%,[12] with strong hydrocarbon-generating abilities. Moreover, there are riverine overlapping sand bodies in the Yangxia Formation, and the oil and gas generated by the source rocks can be stored in tight glutenite nearby. This is why the Yangxia Formation can be used as the main Jurassic production layer in the northern Kuqa of Tarim Basin and why the formation has been a focus of much research.[4,14−16] However, most of the current research has considered the source rock of the coal seam of the Yangxia Formation, and there have been few studies of the coal-bearing tight sandstone in the formation. Hence, it is necessary to further clarify the diagenetic characteristics of the tight sandstone in this formation.

Considering the original sedimentary configuration of the formation, along with the continuation of buried diagenesis, the pore volume of the formation sandstone has gradually decreased and ultimately formed a low-pore, low-permeability sandstone reservoir.[17] In China, tight sandstone is defined as a reservoir with a porosity of less than 10% and a permeability of less than 0.1 mD.[18,19] The diagenetic evolution of tight sandstone and the corresponding pore evolution process are relatively well understood. Sedimentation not only controls the transverse distribution and longitudinal overlapping relationships of sandstone reservoirs but also determines the rock structure characteristics such as particle size, roundness, and sorting of clastic particles in sandstone reservoirs.[20]

Diagenesis is another important factor in the densification of sandstone reservoirs. Mechanical compaction during the early diagenetic stage is the main factor for the extreme deterioration of the physical properties of sandstone reservoirs,[21,22] and cementation diagenesis is an important factor leading to the densification of sandstone reservoirs. Among the many types of cementation, calcareous cementation is the most common and

can be divided into basal cementation during the early diagenetic stage and (iron-containing) cloudy cementation formed during the late diagenetic stage. It is the cementation stage that may lead to extremely poor physical properties of a reservoir if there is limited subsequent dissolution.[22−24] Dissolution is an important factor in improving the reservoir properties of tight sandstones, enabling them to form high-quality reservoirs. As an important source rock in the Yangxia Formation, the coal seam has mainly produced early humic acid and late organic acid, and these two acidic fluids have selectively dissolved different mineral grains within the sandstone during different periods, leading to the non-homogeneity of the diagenetic evolution of the tight sandstone in the region.[25,26]

As massive coal seams were developed near the tight sandstone of the Yangxia Formation, their diagenetic evolution must have been affected by the coal seam fluids. Previous studies have proposed that the diagenetic evolution of the coal-bearing tight sandstone is related to the humic acid produced during the paragenetic to early diagenetic period of the coal seams, which led to the selective dissolution of components in feldspar and detrital particles, reducing the compressive strength of the rock and early compaction of the sandstone.[26,27] However, it remains unclear how the subsequent diagenetic evolution of the tight sandstone near the coal seams evolved further under early tight compaction. Consequently, this study focuses on the impact of coal seam fluids on reservoir heterogeneity and summarizes the characteristics and causes of differential dissolution of coal-bearing tight sandstone and cementation as a result of different dissolution products during different periods. The aim of the study is to systematically summarize the characteristics and causes of diagenetic processes experienced in the Yangxia Formation in the northern Kuqa Depression under the influence of coal seams.

2. GEOLOGICAL BACKGROUND

2.1. Tectonic Setting and Evolution. The Tarim Basin in northern Xinjiang, China, is a Mesozoic foreland basin.[14,15,28] The Kuqa Depression on the northern margin of the Tarim Basin is bounded by the Northern Tarim uplift in the south, the South Tianshan orogen in the north, the Yangxia Depression in the east, and the Wushi Depression in the west (Figure 1). The northeast−southwest trending Kuqa Depression has a length of about 400 km and a width ranging from 30 to 120 km with an area of about 2.8×10^4 km^2.[29,30] The study area is located at the northern end of the Kuqa Depression, and separately, it can be divided into the Dibei Slope Zone and the Tugerming Structural Zone from the west to the east.

From the Paleozoic to the present, the Kuqa Depression has experienced three major tectonic movements: (1) the foreland basin stage from the Late Permian to the Triassic, (2) the rifting and subsidence basin stage in the Jurassic, and (3) the regenerated foreland basin stage after the Cretaceous.[4,15,16] The Yanshan and Xishan periods were the main periods of tectonic activity and fault formation in the Kuqa Depression, with the development of four nearly east−west trending basement detachment thrust faults. These faults control the formation of the "four belts and three depressions" structural pattern in the Kuqa Depression.[15,28]

2.2. Regional Stratigraphic Characteristics. The Lower Jurassic Yangxia Formation in the northern Kuqa Depression is characterized by massive mudstones and coal seams with vertically thick interlayers of sandstone−conglomerates. It can be subdivided into four lithological units from top to bottom, including the carbonaceous mudstone unit, the upper coal-bearing mudstone unit, the sandstone−conglomerate unit, and the lower coal-bearing mudstone unit (Figure 1). The Yangxia Formation is characterized by various sedimentary facies, including lakes, swamps, and braided river deltas. The tight sandstone−conglomerate reservoir is mainly composed of microfacies from distributary channels in the braided river delta plain subfacies and subaqueous distributary channels in the foreland subfacies. Multiple layers of massive mudstone and coal seams were deposited in the overlying and underlying strata of the compact sandstone−conglomerate reservoir. These layers are characterized by high maturity of hydrocarbon source rocks reaching up to 1.5%, average total organic carbon content greater than 2% with a maximum of 38%, pyrolysis hydrocarbon generation potential ranging from 2.5 to 3.5 mg/g, and chloroform asphaltene "A" content ranging from 0.4 to 0.6‰.[9,11,28]

2.3. Coal Seam Distribution. The coal seam in the Yangxia Formation is widely distributed throughout the study area. Although the upper wall of the Yishen 4 well appears to have been affected by a thrust fault, the coal seam of the Yangxia Formation at the bottom of the fault slip layer has been lengthened and thickened longitudinally, and coal seams in other wells were found to be between 7 and 36 m thick. Among these, the average thickness of coal seams in the western Dibei block was 27.8 m, the number of layers was between 5 and 28, and the coal-to-ground ratio was about 6.04%. The average thickness of the coal seam in the eastern Tugelming block was found to be 19.6 m, the number of layers was between 5 and 19, and the coal-to-ground ratio was about 4.61% (Figure 2).
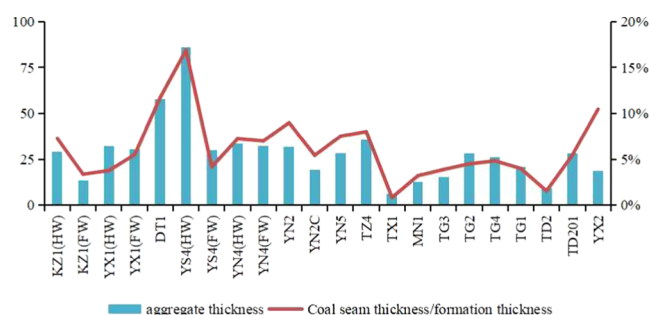

Figure 2. Distribution and combination types of coal seams of the Yangxia Formation in the northern Kuqa Depression.

3. MATERIALS AND METHODS

Samples were collected from 18 wells, including the Yinan 2, Yinan 4, Yinan 5, Tudong 2, Tuge 3, Tuge 4, Dibei 105, Dibei 5, and Yishen 4 wells, and so on, in the north of Kuqa, Tarim Basin (Figure 1). For the tight sandstone reservoir of the Yangxia Formation in the lower Jurassic, 127 sandstone cores were collected and used to prepare thin-section castings for petrographic analysis. And they were first impregnated with a blue resin before thin-section castings were prepared. These thin sections were also partially stained with alizarin red S and potassium ferricyanide for subsequent carbonate mineral differentiation.

In addition to the collected samples, well logging data, completion reports, and routine core test results such as porosity and permeability values were obtained from the PetroChina Tarim Oilfield Company, while other tests were conducted by the National Key Laboratory of Deep Oil and Gas, China University of Petroleum (East China).

3.1. Cathode Luminescence (CL). Cathode luminescence (CL) was used to observe the color characteristics of different types of calcite cement and quartz and to determine the bonding strength and bonding period of calcite cement and quartz cement. It was confirmed that most of the samples in the study area contained siliceous and calcite cement using thin-section identification, and CL was used to distinguish the luminescence characteristics of different origins of the cement. The CL tests were conducted at the National Key Laboratory of Deep Oil and Gas of China, University of Petroleum (East China). The equipment used was a Camera bridge CL 8200 MK 5 detector, with an acceleration voltage of 10 kV, a beam current of 250 mA, an exposure time of 20−60 s, and magnifications of 50, 100, and 200×. The type of calcite cement and its corresponding cathode fluorescence characteristics were further determined through the observation and identification of polished flakes.

3.2. Scanning Electron Microscopy (SEM). In order to better determine the micromorphology of cement and the mineral elements around it, 16 typical sandstone samples containing calcite cement of different phases were selected according to the petrological characteristics of the thin sections. A metal coating was applied to the surface of each sheet before it was used for testing. The metal coating was a nanothick platinum coating, and the spraying process took about 10 s. This operation improved the surface conductivity of the sample and made the image clearer under an electron microscope. The SEM tests used a Crossbeam 550 electron microscope and were conducted in the National Key Laboratory of Deep Oil and Gas of China, University of
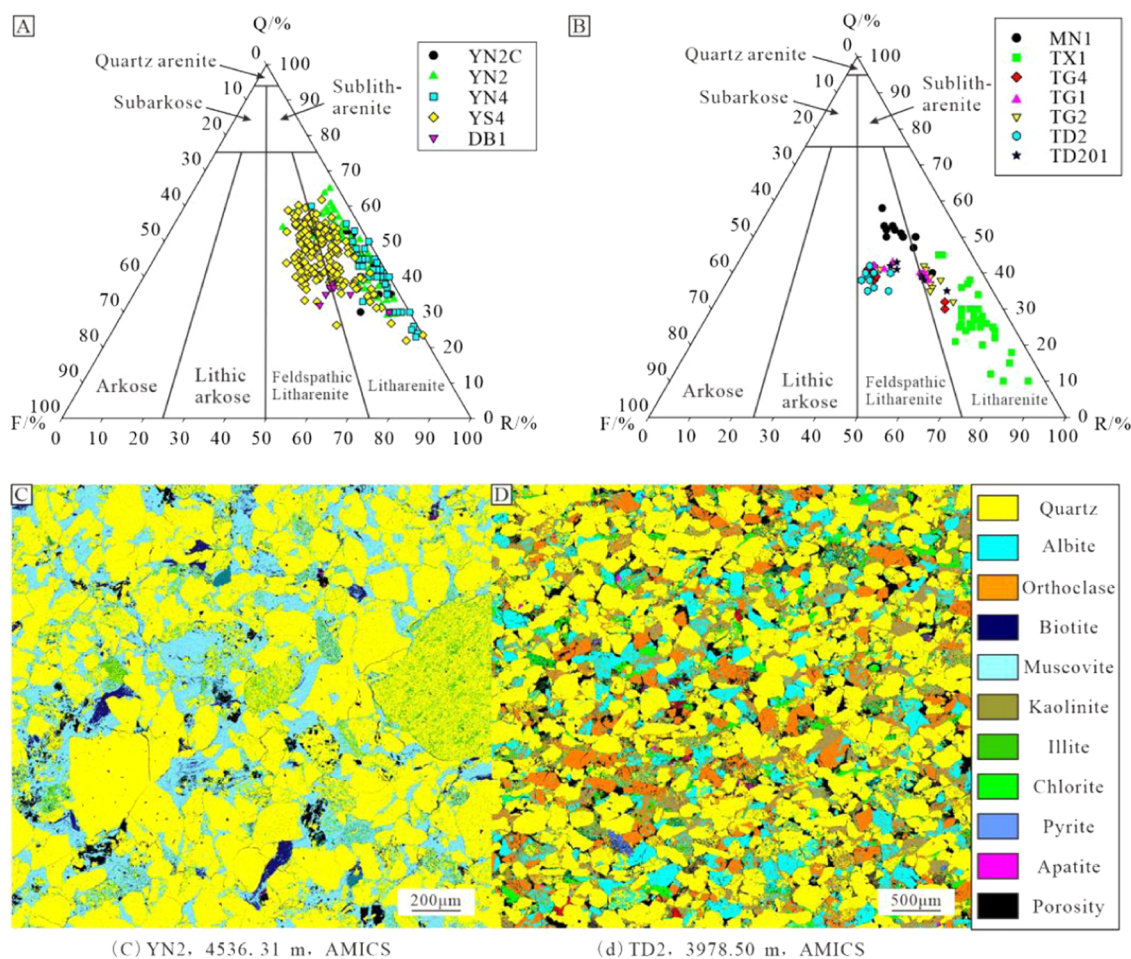
Figure 3. Reservoir components and rock types of the Yangxia Formation. (A) Diagram of minerals of the J^1y sandstone in the Dibei block; (B) diagram of minerals of the J^1y sandstone in the Tugeerming block; (C) AMICS results of the sandstone reservoir in the Dibei block; and (D) AMICS results of sandstone reservoir in the Tugerming block.

Petroleum (East China). The acceleration voltage used was 20 keV, and the magnifications used were 100−10,000×. The chemical elements were characterized semiquantitatively under SEM, and the shape, size, and distribution of pores were identified and characterized.

3.3. Advanced Mineral Identification and Characterization System (AMICS). AMICS scanning analysis and SEM scanning analysis can provide an accurate distribution and content characteristics of diagenetic minerals. A total of 10 typical sandstone samples with obvious diagenesis were selected. Samples were selected for composition analysis using a Bruker AMICS-Mining system and for element distribution analysis using a Bruker Q200-XF 6100. Thin sections were coated with a platinum coating to improve the electrical conductivity of the sample surface. Combined with the BSE image and energy spectrum characteristics, the mineral type, content characteristics, and chemical element composition were accurately identified.

3.4. Carbon and Oxygen Isotopes. Carbon and oxygen isotope analysis can be used to estimate the calcite formation temperature and fluid salinity in order to determine the origin of calcite. In order to reflect the characteristics of tight sandstone reservoirs in this study, combined with the petrographic characteristics, 5 typical sandstone samples containing carbonate cement were selected for carbon and oxygen isotope analysis. The principal analysis device used was

an isotope mass spectrometer host MAT-253, and the sample preparation system was a Kiel Type IV carbonate unit. The experimental conditions were room temperature ranging between 21 and 23 °C, a humidity of about 50%, and a relative humidity of ±5%. The selected samples were all sandstone samples free of organic matter and carbonate cuttings from different wells, different depths, different sequence locations, and different lithologies. The allowable deviation of carbon isotope content test results was ≤±0.1‰, and the allowable deviation of oxygen isotope content was ≤±0.2‰. Stable isotope data of carbon and oxygen were expressed as δ, and the standard for carbon and oxygen isotope analysis was the PDB standard and the SMOW standard obtained from the Lower Cretaceous Pee Dee Formation in South Carolina.

4. RESULTS

4.1. Lithological Characteristics. In the Yangxia Formation of the Dibei area, the average quartz content was found to reach 41.0%, the average feldspar content reached 7.5%, and the average rock cut content reached 42.6%. In the Yangxia Formation of the Tugerming area, the average quartz content reached 36.1%, the average feldspar content reached 15.7%, and the average rock cut content reached 47.2% (Figure 3). The feldspars from the Dibei area were mainly dominated
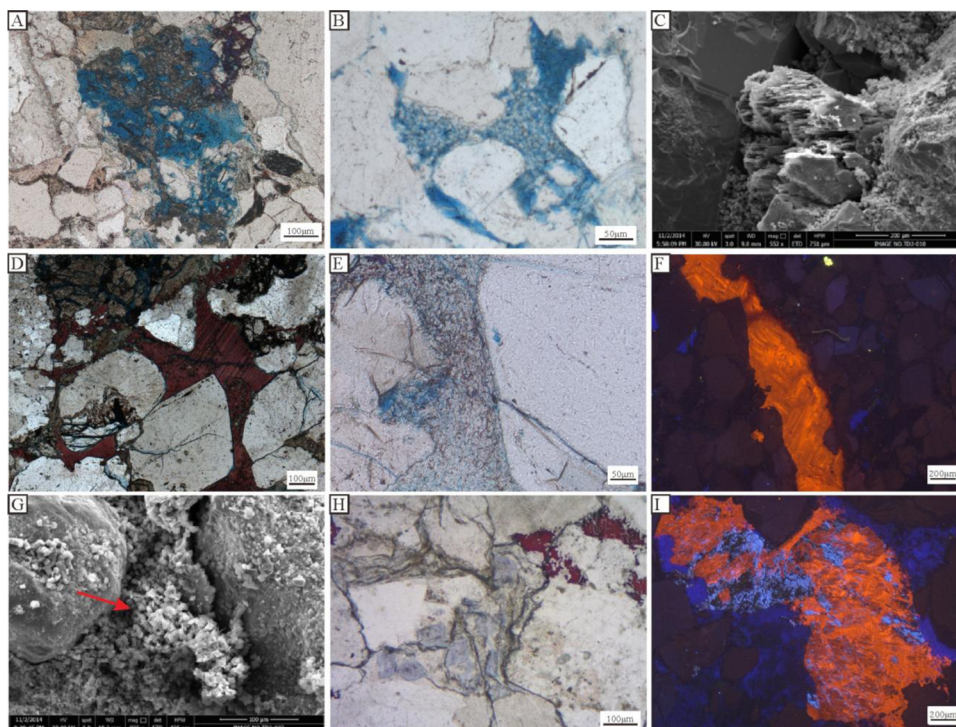
Figure 4. Microscopic diagenetic characteristics of the Yangxia Formation in the northern Kuqa Depression: (A) YS4, 3682.50 m, Feldspar corrosion and siderite cementation; (B) TD2, 3978.90 m, kaolinite fills secondary pores; (C) TD2, 3981.40 m, strong dissolution of potassium feldspar; (D) YN5, 4695.00 m, early calcite basement cement; (E) YS4, 3578.40 m, kaolinite cementation and quartz overgrowth; (F) YN2, 4612.00 m, late calcite metasomatic quartz with enlarged edges; (G) TD2, 3983.18 m, intergranular filled with authigenic kaolinite; (H) YN5, 4693.20 m, ferrodolomite metasomatic illite; and (I) YS4, 3678.25 m, late iron calcite replaced feldspar.

by potassium feldspar with an average content of about 8.8% and plagioclase feldspar with an average content of about 2.9%.

Samples from the Tugermin area exhibited similar characteristics in terms of feldspar types with an average potassium feldspar content of about 12.5% and an average plagioclase feldspar content of 3.2%.

According to the results of the automatic mineral analysis and thin-section statistics (Figure 3), the Yangxia Formation is dominated by lithic sandstone, followed by feldspathic lithic sandstone. From the west to the east, the Yangxia Formation reservoirs gradually transition from lithic sandstone to feldspathic lithic sandstone.

The filler content in the Dibei area in the western part of the Kuqa depression was found to be high, with an average content of 4.0% cement and 5.7% matrix. Muddy matrix was dominant with an average content of about 5.6%, and the cement was dominated by clay minerals and calcareous cement, with an average clay mineral content of about 7.3%, and less siliceous and ferruginous cement.

4.2. Diagenetic Characteristics. *4.2.1. Dissolution.* Reservoir pores observed in the samples from the Yangxia Formation in the northern structural belt of the Kuqa Depression (Figure 4) were mainly secondary pores (Figure 4c). Dissolution microscopic features were mainly dissolution pores formed along the cleavage surfaces. If dissolution is more intense, cleavage fissures were not seen in the feldspar, and only tatted fragments exhibited the original particle shape. There were also intragranular dissolution pores with irregular edges, which were characterized by the shape of a dissolved harbor.

In the Dibei block of the study area, the dissolution effect was found to be relatively strong, and the type of dissolution

particles was mainly feldspar, with a small amount of rock debris and quartz dissolution. A possible reason for the strong dissolution in the Yangxia Formation reservoir in the Dibei block may be the development of tectonic fractures, which have provided acid fluid from coal seams and mudstone. This strengthened the dissolution and improved the physical properties of the reservoir.

In the Tugelming block, due to the shallow depth and weak compaction, a large number of primary pores were found to have been retained and the dissolution effect was found to be weaker than that in the Yangxia Formation in the Dibei Block. However, secondary pores still provided the main reservoir space, forming reservoir space characteristics of secondary and primary pores. Dissolution was found to be strong in the lithologic unit with coarse particles from top to bottom. On the other hand, in the lithologic unit containing many hybrid bases and plastic particles, pore throats were blocked; hence, fluid would find it difficult to enter, and the resulting dissolution became reduced.

4.2.2. Cementation. 4.2.2.1. Quart Overgrowth and Authigenic Quartz. Siliceous cementation was found to be common in the Yangxia Formation in the northern Kuqa Depression, in both the Dibei block and the Tugelming block. Cementation often took the form of quartz overgrowth with small authigenic quartz particles. The small authigenic quartz particles tended to be highly autotypic, with perfectly crystalline hexagonal bipyramidal crystals endowed in intergranular pores. In contrast, quartz overgrowth was often found as hypocrystalline wrapped around the edges of particles. The small authigenic quartz particles and quartz overgrowth were often black under CL and did not emit light. The quartz
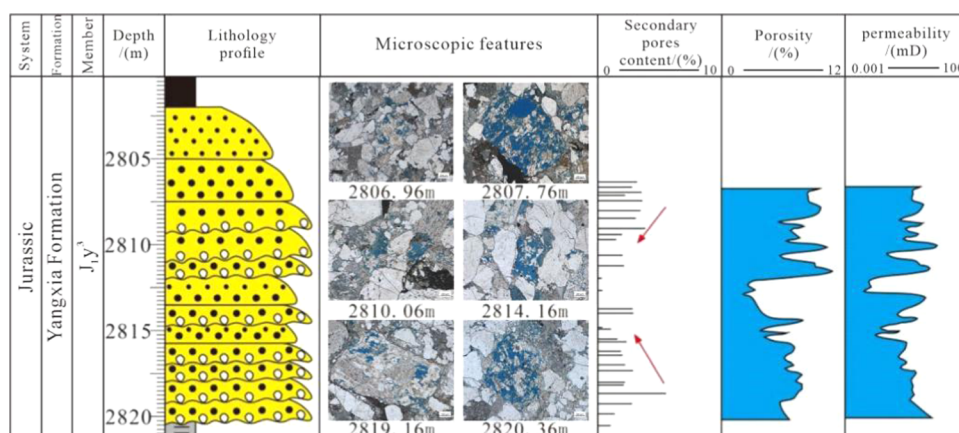
Figure 5. Dissolution intensity distribution of Yishen Well 4.

overgrowth seen in Figure 4e results in a tight reservoir and weakens the development of pores.

4.2.2.2. Calcite Cementation. It was found that carbonate cementation was most developed in the Dibei block, which was often observed as porous or basement cementation. In the Tugelming block, calcite cementation was weak, and porous or basement cementation was not common and often existed as single autotype carbonate particles. Among these, a large amount of symbiosis development of calcite and ferridolomite was seen in well Yinan 5 (Figure 4h). In the Tuge 4 well, the calcite development was banded and filled with structural fractures.
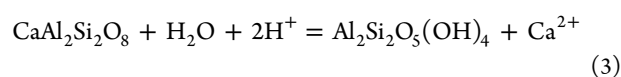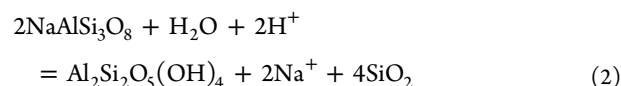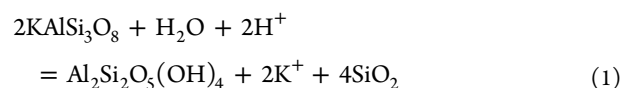
4.2.2.3. Clay Mineral Cementation. Kaolinite is widely distributed in the Yangxia Formation reservoir in the northern Kuqa Depression in the form of book pages or accordions. In the samples from this area, a large number of intercrystal pores were found, providing a reservoir space with high porosity and low permeability (Figure 5). On the plane, authigenic kaolinite is mainly distributed in the Tugelming block, and it is also developed in the Dibei block. Longitudinally, kaolinite filling was found in the shallow part of the formation, and kaolinite gradually transformed into illite as the depth increased. In the transition range of kaolinite to illite, the crystal type was often fuzzy and the intercrystal pores decreased. The illite usually looked scaly, feathery, and wispy under SEM and grew from the edge to the center of pores. Dissolution pores of the feldspar were also seen in the same layer.
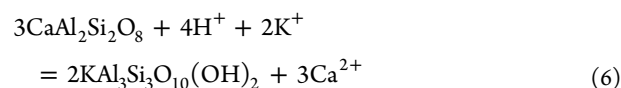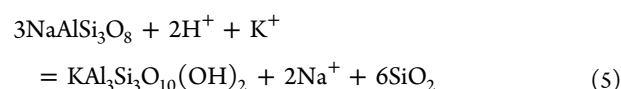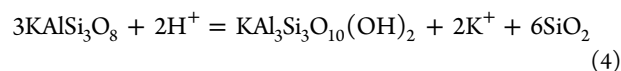
5. DISCUSSION

5.1. Causes of Dissolution of Coal-Bearing Tight Sandstone. It can be assumed that the widely distributed coal seams of the Yangxia Formation discharged rich humic acid and organic acid, modifying the reservoir in multiple stages. It has been pointed out that a large amount of humic acid can be produced early in the burial of coal seams, which selectively dissolves feldspars, rock fragments, and calcareous muds in a reservoir, and the products tend to be highly migratory and can play a purifying role.[26,31,32] With the evolution of the coal seam, a large number of organic acids may have been produced when it entered the low maturity stage ($R_o > 0.5\%$), and the concentration of organic acids in the coal seam fluids probably reached a peak at about 100 °C in the middle orogenic stage, which is the strongest stage of coal dissolution of the sandstone conglomerate.

It was revealed that the dissolution of the Yangxia Formation reservoir in the study area was dominated by feldspar, rock debris, and matrix. Among these, feldspar particles accounted for 69.7% of the most dissolved particles and the proportion of debris and matrix accounted for 30.3%, in which potassium feldspar acid dissolution was the most important type of feldspar dissolution. Feldspar particles often dissolved along cleavages and formed intragranular pores. The feldspar with more intense dissolution could no longer see the cleavage fissures, and only the residue remaining after dissolution revealed the original particle shape.

When feldspar is dissolved, there will be a large number of associated minerals, e.g., kaolinite, quartz, etc., and the specific reaction equation is as follows[33]

$$2KAlSi_3O_8 + H_2O + 2H^+$$
$$= Al_2Si_2O_5(OH)_4 + 2K^+ + 4SiO_2 \tag{1}$$

$$2NaAlSi_3O_8 + H_2O + 2H^+$$
$$= Al_2Si_2O_5(OH)_4 + 2Na^+ + 4SiO_2 \tag{2}$$

$$CaAl_2Si_2O_8 + H_2O + 2H^+ = Al_2Si_2O_5(OH)_4 + Ca^{2+} \tag{3}$$

When the dissolution continues, with the increase of K^+ and Na^+ concentration, potassium feldspar will dissolve and produce illite. The reaction equation is as follows[33]

$$3KAlSi_3O_8 + 2H^+ = KAl_3Si_3O_{10}(OH)_2 + 2K^+ + 6SiO_2 \tag{4}$$

$$3NaAlSi_3O_8 + 2H^+ + K^+$$
$$= KAl_3Si_3O_{10}(OH)_2 + 2Na^+ + 6SiO_2 \tag{5}$$

$$3CaAl_2Si_2O_8 + 4H^+ + 2K^+$$
$$= 2KAl_3Si_3O_{10}(OH)_2 + 3Ca^{2+} \tag{6}$$

Huang et al. explained the dissolution process of different feldspars using thermodynamics. They showed that calcium feldspar is more susceptible to dissolution under near-surface conditions, while potassium feldspar and sodium feldspar do not undergo dissolution until high temperature, and potassium feldspar dissolution is dominant.[32] In the tight sandstone reservoirs of the Yangxia Formation in the Kuqa Depression, rock debris is very rich. Previous studies[3,4,9] have proved that

under the influence of organic acids, volcanic debris is the most prone to dissolution, of which rhyolite debris, andesite debris, and granite debris are the most soluble, followed by gneiss in metamorphic debris, and slate and schist are more difficult to dissolve under the influence of organic acids.[34]

In a thick layer of sandstone with a normal stratigraphic sequence (Figure 5), the content of the dissolution pores in the middle was found to be lower, while the secondary porosity was higher near the top or bottom of the sandstone close to coal seams or mudstones. Thus, it is inferred that the acidic fluids generated by the coal seams had a strong dissolution effect on the reservoir, creating a large number of dissolution pores that improved the physical properties of the reservoir.

Kaolinite and illite produced by the dissolution of feldspar were often found filling secondary pores or transported by fluids and precipitated in the pores of other strata most likely when the system was open due to the tectonic setting. The secondary and residual primary pores became blocked again, thus degrading the physical properties of the reservoir. In addition, the silica produced by feldspar dissolution will have further acted on the reservoir through siliceous cementation in the form of authigenic quartz and quartz overgrowth, thereby, to some extent, destroying the storage space of the reservoir.

On the basis of the Easy% R_o model, the vitrinite reflectance (R_o) value can be calculated as follows[35]

$$W_i/W_{oi} = \exp\left[\int_0^t A\,\exp(-E_i/RT)\mathrm{d}t\right] \tag{7}$$

$$R_o = \exp\left(-1.6 + 3.7\sum_i f_i(1 - W_i/W_{oi})\right) \tag{8}$$

where W_i, W_{oi}, E_i, and f_i represent the residual concentration, original concentration, activation energy, and chemical equivalent coefficient of the participating substance in the ith reaction, respectively; R is the gas constant; T is the formation temperature (absolute temperature); and A is the frequency factor.

The intensity of the dissolution is obviously controlled by the source rocks of the coal seams. Using statistically measured R_o values and calculated R_o values according to the Easy% R_o model (Table 1), it is concluded that the R_o values of the

Table 1. R_o Calculated Values of Each Well Interval

well	depth (m)	temperature (°C)	R_o (%)	dissolution pore (%)
TD2	3974	117.90	0.75	1.53
KZ1	2955	87.80	0.55	0.20
TZ2	4314	132.30	0.88	0.48
YN2C	4690	134.28	0.90	1.80
YN4	4127	125.05	0.81	0.38
YN5	4539	133.49	0.89	2.81
YN5	4595	135.14	0.91	2.50
YS4	2579	79.97	0.50	1.56
YS4	2733	84.29	0.51	0.10
YS4	2801	86.20	0.52	2.65

source rock of coal seams in the Yangxia Formation of the Kuqa Depression are mostly distributed between 0.5 and 1.3% (Figure 6). The thermal evolution degree is evidently low, the coal belongs to the lignite-gas coal type, and the corresponding diagenetic segment belongs to the meso-diagenetic stage A ∼ meso-diagenetic stage B. On the basis of the correlation
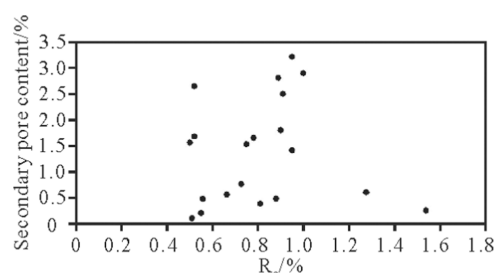

Figure 6. Relationship between R_o values and dissolution pore content in the Yangxia Formation of the Kuqa Depression.

between coal seam maturity and the secondary porosity contents in the sandstone reservoir within a limited range (<12 m) from the coal seam (Figure 6), it can be observed that the content of secondary pores does not always increase with the increase of R_o of the coal seam. The R_o of most strata of the Yangxia Formation is greater than 0.5%, the corresponding coal seam has entered the mature stage (long bituminous coal), and the humic acid in the coal seam and nearby strata has been decomposed. The content of organic carboxylic acids began to increase. When R_o was between 0.5 and 1.0%, the content of organic carboxylic acid gradually increased to the peak. When R_o > 1.0% and the formation temperature is higher than 100−120 °C, binary organic acids and mono organic acids begin to decompose in turn, the overall yield of organic carboxylic acid in the coal seam begins to decline, and the acidic fluid content decreases. Due to the continuous burial depth and the transformation of the fluid from acid to alkaline, the pores not only need to be compressed to reduce the space but also because of the strong sealing property, the products after the dissolution effect will have various cementation and filling effects under the condition of fluid property transformation and poor seepage conditions. Therefore, the content of the secondary pores between particles gradually decreases.

5.2. Causes of Cementation in Coal-Bearing Tight Sandstone. The influence of cementation on the reservoir properties is destructive. During the diagenetic process, due to the change in formation water quality, various ions in the formation fluid combine with each other and cementation occurs in the pores between detrital particles, occupying the reservoir space and leading to the deterioration of reservoir permeability. There are two types of cementation associated with coal seams. One is due to the products of the dissolution of tight sandstone skeleton particles by acid fluid produced by the coal seam, which precipitates in the form of siliceous and kaolinite or illite. The other is due to the CO_2 produced during the thermal evolution of coal seams, which combines with Ca^{2+} and other ions such as Fe^{2+} from other sources and precipitates in the form of calcite and siderite.

Two phases of acid fluid will be produced due to the thermal evolution of a coal seam. When seepage conditions are good, acidic fluid can readily enter the reservoir and dissolve skeletal mineral particles, such as feldspar. Resulting dissolution products can also readily move out of the reservoir. On the other hand, dissolution products will precipitate in secondary pores and residual primary intergranular pores.

In the coal-bearing tight sandstone reservoir with a large burial depth, dissolution mainly occurred in potassium feldspar, and the dissolution of potassium feldspar had a very close relationship with the precipitation of quartz, illite, and kaolinite (eqs 1 and 4). In this study, microscopic observations
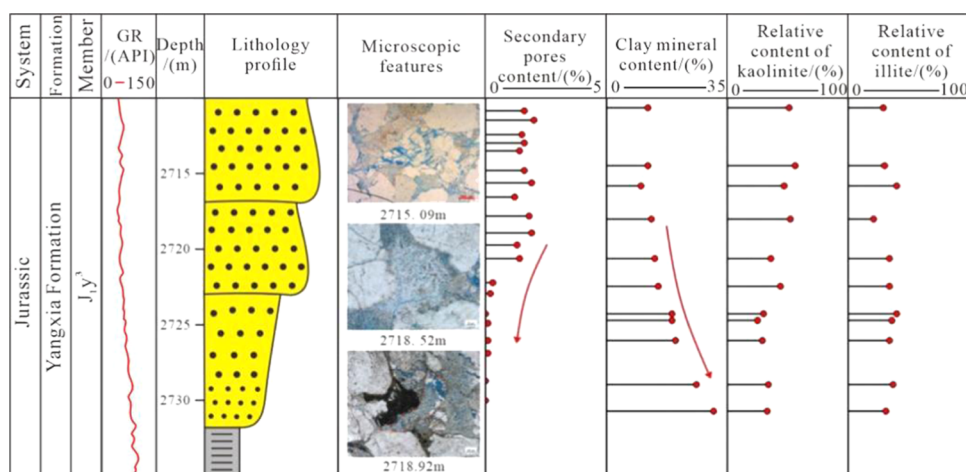
Figure 7. Relationship between clay minerals and the dissolution pore distribution.
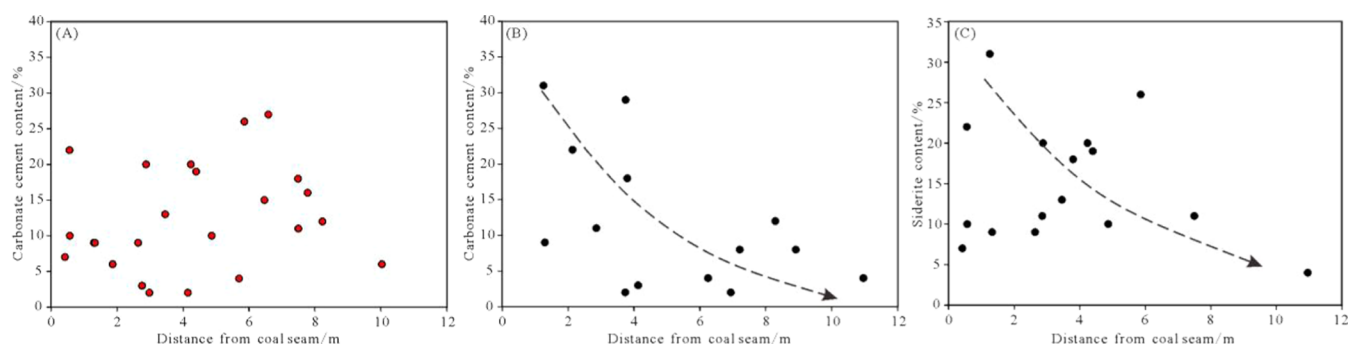

Figure 8. Relationship between carbonate cement content and distance from the coal seam. (A) Relationship between carbonate cement content and distance from the coal seam in the rigidity-rich granular sandstone; (B) relationship between carbonate cement content and distance from the coal seam in the plasticity-rich granular sandstone; and (C) relationship between siderite content and distance from the coal seam.

revealed that quartz was often cemented around the periphery of particles in the form of siliceous overgrowth, with kaolinite accounting for the feldspar as well as filling pores. It can be seen from the relationship between clay minerals and secondary pore content (Figure 7) that when the lithology was from medium coarse sandstone to fine siltstone vertically, the content of secondary pores decreased significantly and the content of clay minerals increased. This suggests that in sandstone with coarse grain size, seepage conditions were better and clay minerals migrated easily. When the grain size became finer or when it was blocked by finer-grained mudstone, it was difficult for clay minerals to migrate and easier for them to precipitate.

Debris components have an innate control over reservoir quality, which can cause differences in diagenesis between different reservoirs during the early burial stage. Quartz, feldspar, and other skeleton mineral particles are rigid particles with strong compressive resistance, while mica and plastic debris are plastic particles with weak compressive resistance. Therefore, according to the different contents of clastic particles, sandstone can be divided into rigidity-rich granular sandstone or ductile-rich lithic sandstone.

The relationship of siderite cement with the distance from the coal seam is different from that of carbonate cement in the rigidity-rich granular sandstone as the high-value point of siderite cement lies closer to the coal seam (Figure 8b). Siderite cementation often occurs in the early stage of compaction, and the zone with high content is often close to

the coal seam. Due to the change in water properties, a large amount of $Fe(OH)_2$ was deposited in the water, and the $Fe(HCO_3)_2$ solution generated by the interaction with CO_2 produced by early organic matter was most likely precipitated into siderite precipitation in a slightly alkaline environment.[36,37] In contrast, the distribution of siderite cement was similar to that of carbonate cement in ductile-rich lithic sandstone. This suggests that the ductile-rich lithic sandstone was conducive to the formation of a slightly alkaline water environment and that cementation occurred during the early burial stage, thus occupying the intergranular pores. In addition, the plastic particles had weak compression resistance, so ductile-rich lithic sandstone could densify earlier than rigidity-rich lithic sandstone, which affected the infiltration of acidic fluids during the later stage and weakened the dissolution strength of acidic fluids on the reservoir.

Considering that coal seams produce a large amount of humic acid during the early diagenetic stage, the sandstone near the coal seam experienced leaching from the coal seam first under good seepage conditions, resulting in the dissolution of calcareous debris and intergranular calcareous mud in the upper part of the large set of positive-grained sand conglomerate. The content of carbonate cement in this region is low. Subsequently, calcium-containing fluid flowed into the conglomerate, and carbonate cementation occurred when the CO_2-containing fluid entered the reservoir,[38-40] and the cementation content decreased with increasing distance from the coal seam. With the increase of temperature of the organic
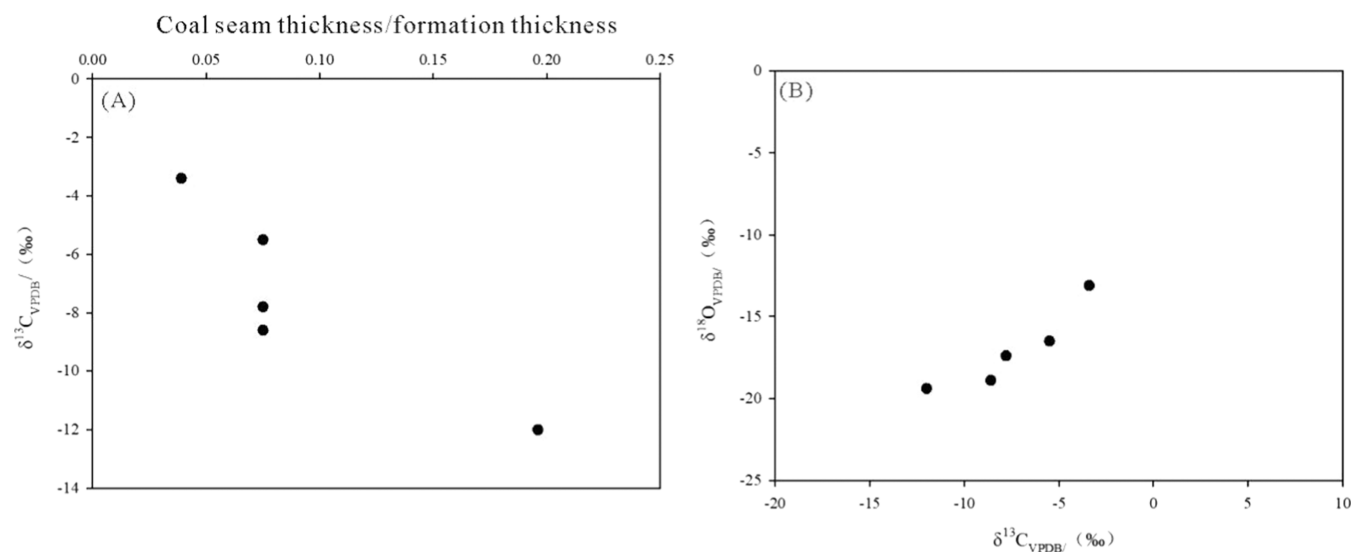
Figure 9. Carbon and oxygen isotope analysis. (A) Relationship between carbon isotope characteristics and the ratio of coal seam thickness to formation thickness and (B) carbon and oxygen isotope characteristics of the Yangxia Formation.

Table 2. Recovery of Paleotemperature and Paleosalinity of Calcite Cementation

well	depth (m)	$\delta^{13}C_{VPDB}$ (‰)	$\delta^{18}O_{VPDB}$ (‰)	main minerals	paleosalinity (Z)	paleotemperature (°C)
YS4	3678.25	−3.4	−13.1	calcite	113.81	87.52
YS4	4127.4	−12.0	−19.4	calcite	93.06	140.24
YN5	4692	−8.6	−18.9	calcite	100.28	135.68
YN5	4692.5	−5.5	−16.5	calcite	107.82	114.69
Yn5	4694.2	−7.8	−17.4	calcite	102.66	122.39

acid production again during the middle diagenetic stage, it easily dissolved soluble minerals and carbonate cement. When kerogen entered the high/overmature stage, a large amount of CO_2 was produced, altering the fluid to meet conditions for carbonate cement precipitation.

The organic acids and carbon dioxide released during the thermal evolution of source rocks can affect calcium precipitation and control the carbon isotopes in calcareous cement. The eigenvectors of carbon isotopes from organic sources are very low, ranging from −18 to −33‰.[42] According to the carbon and oxygen isotopes of the calcareous cement found in this study (Figure 9), the carbon and oxygen isotopes in the Yangxia Formation reservoir in the northern Kuqa Depression had obvious negative values, and the larger the coal-to-ground ratio, the lower the eigenvector of the carbon isotopes. Hence, it is inferred that the ligand is closely related to organic matter.

Using the eigenvectors of carbon and oxygen isotopes, the paleotemperature and paleosalinity at the time of cementation can be estimated to provide information about the cementation period and precipitation conditions. The paleotemperature can be calculated as follows[43]

$$1000 \ln \alpha_{calcite-water} = 2.78 \times 10^6 / T^2 - 2.89 \quad (9)$$

$$\alpha_{calcite-water} = \frac{(1 + (\delta^{18}O_{calcite}/1000))}{(1 + (\delta^{18}O_{fluid}/1000))} \quad (10)$$

where $\alpha_{calcite-water}$ is the ratio of isotopes between two different substances. The $\delta^{18}O_{fluid}$ and $\delta^{18}O_{calcite}$ are both PDB standards. Since the sedimentary period of the Yangxia Formation occurred during the presence of a continental

freshwater environment, $\delta^{18}O_{water}$ is taken as that of mixed Jurassic seawater and atmospheric freshwater, with a value of −2.5‰.[44] The conversion of the SMOW standard to the PDB standard is based on the formula recommended by the US Geological Survey,[45]

$$\delta^{18}O_{SMOW} = 1.03086 \cdot \delta^{18}O_{PDB} + 30.86 \quad (11)$$

The calculation formula of paleosalinity is[46]

$$Z = 2.048 \cdot (\delta^{18}C + 50) + 0.498 \cdot (\delta^{18}O + 50) \quad (12)$$

Calcite cementation from the Yishen 4, Yinan 4, and Yinan 5 wells was used to measure carbon and oxygen isotopes (Table 2), and paleotemperatures and paleosalinities were estimated using the formulas above. These suggest that at least two phases of cementation occurred affecting the calcite cement: low temperature characterizes early cementation with paleotemperatures lower than 90 °C, while high temperatures characterize late cementation with paleotemperatures of 110−140 °C.

Previous studies have shown that the cumulative CO_2 production rate of coal-bearing source rocks is high and relatively stable during the high-overmature stage ($R_o > 1\%$).[47,48] The carbonate colluvium of the sandstone reservoirs located near the coal seams observed in this study derived its carbonaceous quality mainly from CO_2 produced by the coal seams through casein decarboxylation within the oil-generating window. It can be inferred that the reservoir of the Yangxia Formation in the northern Kuqa Depression developed a large amount of calcite cement during the early diagenetic stage. In the coal seam, kerogen will first form a large amount of organic acid through decarboxylation. Then, the kerogen is deoxygenated and carboxyl anions are decarboxylated to produce
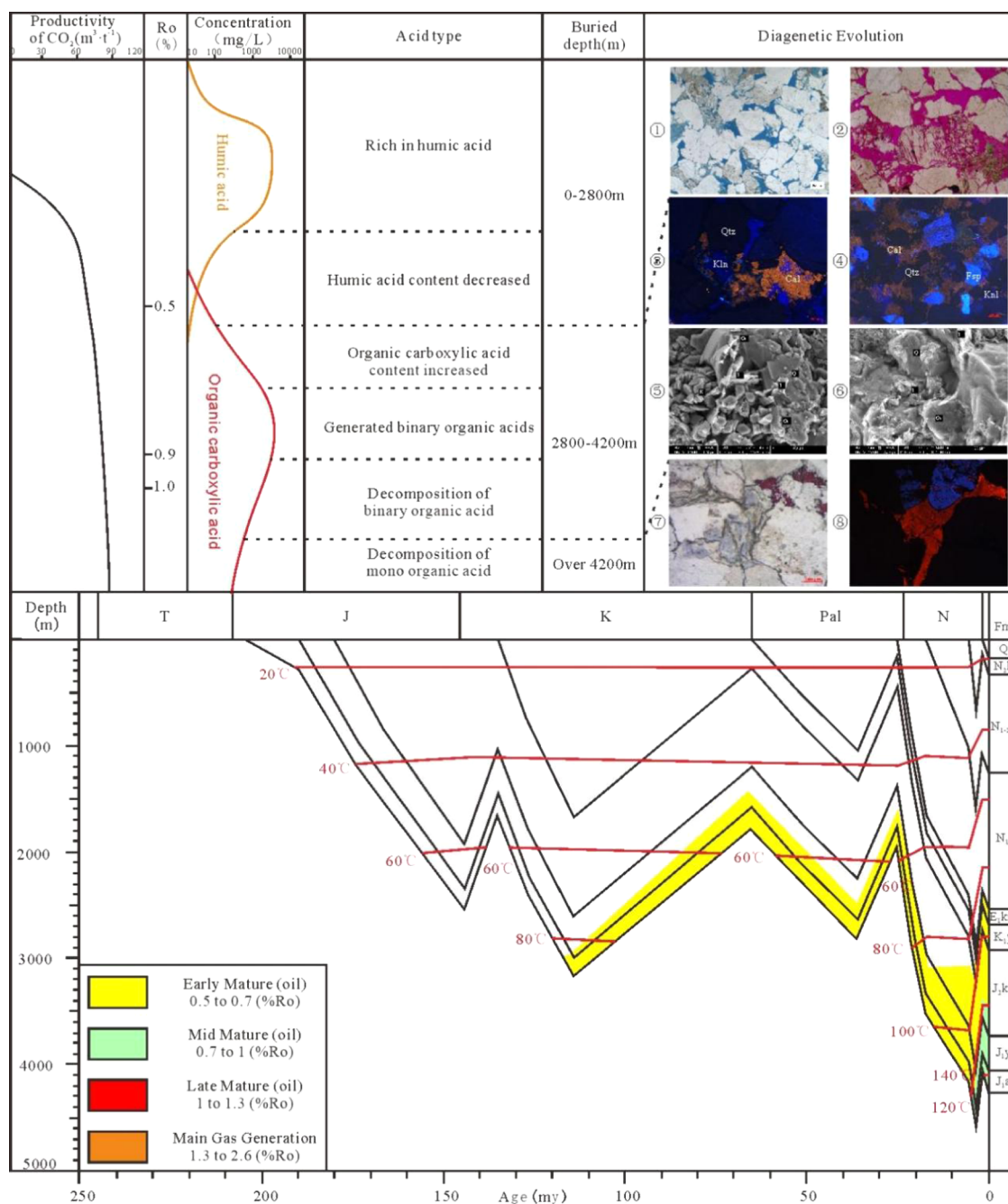
Figure 10. Proposed evolution of the coal-bearing reservoir in the Yangxia Formation, Tarim Basin, northwest China [Refer to Meng et al. for acid concentration curves; Reprinted in part with permission from ref 26. Copyright (2022) Natural Gas Geoscience].[26] ① TD2, 3977.9 m, due to the role of overpressure, is similar to ② MN1, 782.63 m, with less interstitial material between mineral particles. ③ YS4, 3678.25 m, and ④ YS4, 3436.3m, calcitylene basement cementation showed orange cathode luminescence, and the calculated carbon and oxygen isotope temperature was about 87.52 °C. In the same period, kaolinite was filled with pores in situ, reflecting the fact that cement could not move out in time after further compaction of the formation. ⑤ TG4, 3568.73 m, and ⑥ TG4, 3566.85 m, the dissolved potassium feldspar and its products kaolinite and autogenetic quartz can be seen under the electron microscope, and some of the dissolved products of potassium feldspar are illite. ⑦ YN5, 4693.2 m (left) in Yinan, and ⑧ YN5, 4692 m (right), the late calcite appears dark red under cathodoluminescence, and the kaolinite phenomenon of late ferrodolomite replacement illite can be seen.

CO_2 gas, and CO_2 enters solution leading to a decrease in pH in the formation fluid. The fluid mixture of organic and inorganic acids then provides a reliable source of calcium through the dissolution of feldspar, calcareous minerals, and rock debris. Liu concluded, from a simulation experiment on the solubility of minerals under the action of CO_2 fluid,[49] that the solubility of anorthite is higher than that of quartz, potassium feldspar, and albite with a solubility of 200−350 mg/L at 25−50 °C, which is significantly higher than that of other skeleton minerals (<50 mg/L). Huang et al. also explained the dissolution processes in different feldspar using thermodynamics. They showed that anorthite is more prone to dissolution in near-surface conditions, while potassium feldspar and albite can be better preserved in the burial process. The main dissolution of potassium feldspar appears until the temperature is high.[50] In conclusion, the massive dissolution of

early anorthite is also one of the sources of Ca^{2+} in carbonate cements.

5.3. Reservoir Diagenetic Evolution. Combined with the results of previous studies on sedimentology, reservoir development, diagenesis, coal seam evolution in other areas, and previous laboratory simulation results in the study area, a diagenetic evolution model of the coal-bearing reservoir can be proposed (Figure 10).

After a large number of higher plant remains are buried, they can be affected by oxidation and decomposition caused by microorganisms during the shallow burial stage (R_o < 0.5%), producing a large amount of humic acid. As a result, the pH of the fluid medium will be acidic with pH values between 4 and 5.[38] Due to these conditions, feldspar, volcanic rock debris, and carbonate rock debris are dissolved, particle surfaces are purified, and calcareous mud deposited with it is difficult to retain. At this time, seepage conditions are good, and dissolution products move out completely in the form of solutions.

Subsequently, aluminosilicate minerals in skeleton particles continue to dissolve, providing various metal cations such as Ca, Na, K, and Mg to the diagenetic fluid.[41] However, with the reduction of the humic acid content and the long-term diagenetic depletion, the water medium gradually becomes moderately alkaline.

At this time, compaction increases, contact between particles becomes closer, and the cementation of solution products occurs in places where seepage conditions are poor. At this stage, kaolinite and early calcite cemented intergranular primary porosity is common, silicon migration ability is weak, and the silicon is often filled in the form of authigenic quartz particles in the pores of feldspar, with well-defined crystal shapes. With increasing burial depth, the organic matter in the main source layer gradually enters a mature stage (0.5 < R_o < 1.0%). At this point, the coal seam begins to produce large amounts of organic acids, which selectively dissolve the skeletal mineral particles in the reservoir. During this burial depth stage, the potassium feldspar content is high and dissolution is most likely to occur, with the main dissolution object during this stage being potassium feldspar. Without the influence of late cracks, due to the relatively closed space of the system, dissolution products cannot be effectively exported in time, and most of these are cemented within the pores with poor seepage conditions in the form of kaolinite or secondary quartz. At this stage, a large number of in situ precipitation and secondary pores generated by the dissolution of filled original minerals can also be seen.

When the vitrinite reflectance R_o > 1.0%, binary organic acid and mono organic acid begin to decompose successively, and the formation fluid gradually becomes more alkaline, providing good conditions for the cementation precipitation of late ferric calcite and ferric dolomite. A large amount of CO_2 and Ca^{2+} ions produced by dissolution in the old coal seam can be used as the material basis for late calcareous cementation. With the increase in temperature and pressure, the reaction related to the formation of kaolinite gradually changes to a reaction related to the formation of illite.

6. CONCLUSIONS

(1) The coal-bearing tight sandstone of the Yangxia Formation in the northern Kuqa Depression is dominated by lithic sandstone, followed by feldspathic lithic sandstone. The maturity of coal seams in the Yangxia Formation of the Kuqa Depression is mostly between 0.5 and 1.08%, and the highest is 1.5%. At this age, the formation will be characterized by organic carboxylic acid, microscopically visible dissolution pores of potassium, feldspar, and volcanic rock debris.

(2) The coal seams have both constructive and destructive effects on the development of reservoir properties. On the one hand, coal seams provide organic acids to the reservoir, increasing the dissolved pores. On the other hand, dissolution products migrate to precipitate in spaces with poor seepage capacity, clogging primary pores, as well as previously dissolved pores. The large amount of CO_2 generated from coal seams, combined with Ca^{2+} plasma from dissolution, leads to carbonate cementation and promotes further densification of the reservoir.

(3) During the shallow burial stage (R_o < 0.5%), a large amount of humic acid is produced in the coal seam, which causes the dissolution of calcium feldspar and volcanic rock debris, the surfaces of the particles are purified, and dissolution products are moved out completely. When the water gradually becomes moderately alkaline, the cementation of early calcite begins. With increasing burial depth, the organic matter of the main source layer gradually enters the mature stage, and the coal seam begins to produce organic acids, which selectively dissolve the skeleton mineral particles of the reservoir, and the dissolution products cement with kaolinite or illite. When the vitrinite reflectance R_o is more than 1%, binary organic acid and mono organic acid begin to decompose, and the fluid gradually becomes alkaline again, which provides a good condition for late ferric calcite and ferric dolomite cemented precipitation.

■ AUTHOR INFORMATION

Corresponding Author

Wenhao Xia − *National Key Laboratory of Deep Oil and Gas, China University of Petroleum (East China), Qingdao 266580, China;* ⊙ orcid.org/0009-0005-4071-4061; Email: xiawenhao0709@163.com

Authors

Huajun Guo − *Petrochina Hangzhou Research Institute of Geology, Hangzhou 310023, China*

Xiang Shan − *Petrochina Hangzhou Research Institute of Geology, Hangzhou 310023, China*

Kelai Xi − *National Key Laboratory of Deep Oil and Gas, China University of Petroleum (East China), Qingdao 266580, China*

Bo Peng − *Petrochina Hangzhou Research Institute of Geology, Hangzhou 310023, China*

Xianzhang Yang − *Research Institute of Exploration and Development Petrochina Tarim Oilfield Company, Korla 841000, China*

Zhiwen Zou − *Petrochina Hangzhou Research Institute of Geology, Hangzhou 310023, China*

Wenfang Yuan − *Research Institute of Exploration and Development Petrochina Tarim Oilfield Company, Korla 841000, China*

Complete contact information is available at:

Notes

The authors declare no competing financial interest.

■ ACKNOWLEDGMENTS

■ REFERENCES

(1) Spencer, C. W.; Mast, R. F. *Geology of Tight Gas Reservoir*; American Association of Petroleum Geologists, 1986; pp 10−50.

(2) Holditch, S. A. Tight gas sands. *J. Pet. Technol.* **2006**, *58* (6), 86−93.

(3) Huang, W.; Zhang, H.; Xiao, Z.; Yu, S.; Pan, C. Generation, expulsion and accumulation of diamondoids, aromatic components and gaseous hydrocarbons for gas fields in Kuqa Depression of the Tarim Basin, NW China. *Mar. Pet. Geol.* **2022**, *145*, No. 105893, DOI: 10.1016/j.marpetgeo.2022.105893.

(4) Wang, K.; Xiao, A.; Cao, T.; Zhang, R.; Wei, H.; Yu, C. Geological structures and petroleum exploration fields of the northern tectonic belt in the Kuqa depression, Tarim basin. *Acta Geol. Sin.* **2022**, *96* (2), 368−386.

(5) Ali, K.; Rahim, K. *Tight Sandstones: Overview, Distribution, and Global Significance, Reservoir Characterization of Tight Gas Sandstones*; Elsevier, 2022; Chapter 1, pp 1−22.

(6) Caineng, Z.; Zhang, G.; Tao, S.; Hu, S.; Li, X.; Li, J.; Dong, D.; Zhu, R.; Yuan, X.; Hou, L.; Zhai, H.; Zhao, X.; Jia, J.; Gao, X.; Guo, Q.; Wang, L.; Li, X. Geological features, major discoveries and unconventional petroleum geology in the global petroleum exploration. *Pet. Explor. Dev.* **2010**, *37* (2), 129−145.

(7) Kang, Y. Characteristics of tight hydrocarbon reservoirs in China. *Nat. Gas Ind.* **2012**, *32* (5), 1−4.

(8) Hu, S.; Zhu, R.; Wu, S. Profitable exploration and development of continental tight oil in China. *Pet. Explor. Dev.* **2018**, *45* (4), 737−748.

(9) Wang, K.; Yang, H.; Li, Y.; Zhang, R.; Ma, Y.; Wang, B.; Yu, C.; Yang, Z.; Tang, Y. Geological characteristics and exploration potential of the northern tectonic belt of Kuqa depression in Tarim Basin. *Acta Pet. Sin.* **2021**, *42* (7), 885−905.

(10) Gao, T.; Ding, X.; Yang, X.; Chen, C.; Xu, Z.; Liu, K.; Zhang, X.; Cao, W. Geochemical Characteristics and Depositional Environment of Coal-Measure Hydrocarbon Source Rocks in the Northern Tectonic Belt, Kuqa Depression. *Appl. Sci.* **2022**, *12* (19), No. 9464, DOI: 10.3390/app12199464.

(11) Zhao, W.; Zhang, S.; Wang, F.; Cramer, B.; Chen, J.; Sun, Y.; Zhang, B.; Zhao, M. Gas systems in the Kuche Depression of the Tarim Basin:sourceRock distributions, generation kinetics and gas accumulation history. *Org. Geochem.* **2005**, *36*, 1583−1601.

(12) Zhao, G.; Li, X.; Liu, M.; Li, J.; Liu, Y.; Zhang, X.; Zhang, X.; Wei, Q.; Wei, Q.; Xiao, Z. Accumulation characteristics and controlling factors of the Tugeerming gas reservoir in the eastern Kuqa Depression of the Tarim Basin, northwest China. *J. Pet. Sci. Eng.* **2022**, *217*, No. 110881, DOI: 10.1016/j.petrol.2022.110881.

(13) Liu, J.; Yang, X.; Liu, K.; Xu, Z.; Jia, K.; Zhou, L.; Wei, H.; Zhang, L.; Wu, S.; Wei, X. Differential hydrocarbon generation and evolution of typical terrestrial gas-prone source rocks:An example from the Kuqa foreland basin, NW China. *Mar. Pet. Geol.* **2023**, *152*, No. 106225, DOI: 10.1016/j.marpetgeo.2023.106225.

(14) Xing, E.; Pang, X.; Xiao, Z.; Zhang, B.; Jiang, Z.; Li, F.; Guo, J.; Ma, Z. Type discrimination of Yinan 2 gas reservoir in Kuqa depression,Tarim Basin. *J. China Univ. Pet., Ed. Nat. Sci.* **2011**, *35* (6), 21−27.

(15) Peng, W. *Hydrocarbon Accumulation Characteristics and Distribution Patterns in Deep and Shallow Basin in Kuqa Depression, Tarim Basin*; China University of Petroleum: Beijing, 2016; pp 38−54.

(16) Zhang, Y. *Study on the Characteristics of Tight Sandstone Reservoir of Middle-Lower Jurassic in the Eastern Part of Kuqa Depression*; Chengdu University of Technology, 2018; pp 10−15.

(17) Li, Y.; Jia, A.; He, D. Control factors on the formation of effective reservoirs intight sands: examples from Guangan and Sulige gasfields. *Acta Pet. Sin.* **2013**, *34* (1), 71−82.

(18) Dai, J.; Ni, Y.; Wu, X. Tight gas in China and its significance in exploration and exploitation. *Pet. Explor. Dev.* **2012**, *39* (3), 277−284.

(19) Zou, C.; Zhu, R.; Liu, K.; Su, L.; Bai, B.; Zhang, X.; Yuan, X.; Wang, J. Tight gas sandstone reservoirs in China: characteristics and recognition criteria. *J. Pet. Sci. Eng.* **2012**, *88−89* (2), 82−91.

(20) Qin, S.; Wang, R.; Shi, W.; Geng, F.; Luo, F.; Li, G.; Li, J.; Zhang, X.; Ostadhassan, M. Integrated controls of tectonics, diagenesis and sedimentation on sandstone densification in the Cretaceous paleo-uplift settings, north Tarim Basin. *Geoenergy Sci. Eng.* **2021**, *233*, No. 212561.

(21) Worden, R. H.; Burley, S. D. Sandstone Diagenesis: The Evolution of Sand to Stone. In *Sandstone Diagenesis: Recent and Ancient*; Burley, S. D.; Worden, R. H., Eds.; Blackwell Publishing Ltd.: Oxford, United Kingdom, 2003; pp 3−46.

(22) Khan, M. A.; Khan, T.; Ali, A.; Bello, A. M.; Radwan, A. E. Role of depositional and diagenetic controls on reservoir quality of complex heterogenous tidal sandstone reservoirs: An example from the Lower Goru formation, Middle Indus Basin, Southwest Pakistan. *Mar. Pet. Geol.* **2023**, *154*, No. 106337.

(23) Zhixue, S.; Sun, Z.; Lu, H.; Yin, X. Characteristics of carbonate cements in sandstone reservoirs: A case from Yanchang Formation, middle and southern Ordos Basin, China. *Pet. Explor. Dev.* **2010**, *37* (5), 543−551.

(24) Shi, Z.; Li, X.; Dong, D.; Qiu, Z.; Hu, B.; Liang, P. Diagenesis and pore evolution of tight sandstone reservoir: a case study from the Upper Triassic reservoir of the southwest Sichuan Basin, China. *Earth Sci. Front.* **2018**, *25* (2), 179−190.

(25) Li, M. *Study on the Diagenesis-Pore Evolution Difference and Mechanism of Tight Sandstones in Coal Measures*; China University of Mining and Technology, 2020; pp 121−124.

(26) Meng, X.; Dou, Y.; Song, B.; Chen, Y.; Chen, X.; Li, Y.; Peng, B.; Yi, J. Genetic type of coal seams and its control on pore evolution of coal-glutenite: Case study of Badaowan Formation in Mahu area, Junggar Basin. *Nat. Gas Geosci.* **2022**, *33* (11), 1768−1784.

(27) Wu, Y. Coal seam-A genetic stratigraphic sequence boundary in nonmarine basin. *Acta Pet. Sin.* **1995**, *17* (4), 28−34.

(28) Song, X. *Cretaceous Paleo-Uplift Restoration and Its Implications on Hydrocarbon Accumulation in the Kuqa Depression*; China University of Petroleum: Beijing, 2018; pp 68−77.

(29) Dong, X.; Mei, L.; Quan, Y. Types of tight sand gas accumulation and its exploration prospect. *Nat. Gas Geosci.* **2007**, *18* (3), 351−355.

(30) Li, F.; Jiang, Z.; Li, Z.; Wang, X.; Du, Z.; Luo, X.; Xin, S. Enriched Mechanism of Natural Gas of Lower Jurassic in Dibei Area, Kuqa Depression. *Earth Sci.* **2015**, *40* (9), 1538−1548.

(31) Manning, D. A. C. Acetate and propionate in landfill leachates: Implications for the recognition of microbiological influences on the composition of waters in sedimentary systems. *Geology* **1997**, *25* (3), 279−281.

(32) Huang, S.; Huang, K.; Feng, L.; Tong, H.; Liu, L.; Zhang, X. Mass exchanges among feldspar, kaolinite and Illite and their influences on secondary porosity formation in clastic diagenesis—A case study on the Upper Paleozoic, Ordos Basin and Xujiahe Formation, Western Sichuan Depression. *Geochimica* **2009**, *38* (5), 498−506.

(33) Sun, G.; Wang, Z.; Liu, P.; Zhang, Z. Dissolved micro-pores in alkali feldspar and their contribution to improved properties of tight sandstone reservoirs: A case study from Triassic Chang-63 sub-

member, Huaqing area, Ordos Basin. *Oil Gas Geol.* **2022**, *43* (3), 658−669.

(34) Cao, Yi.; Wang, Q.; Qu, X.; Wang, G.; Miao, C.; Gao, Y.; Chen, S. A dissolution experiment of organic acid of cuttings and its verification: a case study of the Dongying Formation of the CFD6−4 oilfield, Bozhong sag. *Acta Pet. Sin.* **2020**, *41* (7), 841−852.

(35) Sweeney, J. J.; Burnham, A. K. Evaluation of a simple model of vitrinite reflectance based on chemical kinetics. *AAPG Bull.* **1990**, *74* (10), 1559−1570.

(36) Shen, Y.; Qin, Y.; Li, Z.; Jin, J.; Wei, Z.; Zheng, J.; Zhang, T.; Zong, Y.; Wang, X. The sedimentary origin and geological significance of siderite in the Longtan Formation of western Guizhou Province. *Earth Sci. Front.* **2017**, *24* (6), 152−161.

(37) Li, B.; Li, J.; Yang, K.; Ren, C.; Xu, J.; Gao, Z. Evolution law of coal permeability based on comprehensive effect of pore pressure and water. *J. China Univ. Min. Technol.* **2020**, *49* (1), 44−53.

(38) Zheng, J.; Ying, F. Reservoir characteristics and diagenetic model of sandstone intercalated in coal-bearing strata (acid water medium). *Acta Pet. Sin.* **1997**, *18* (4), 19−24.

(39) Cao, Y.; Chen, L.; Wang, Y.; Sui, F. Diagenetic evolution of Es3 reservoir and its influence on property in the northern Minfeng sub-sag of Dongying sag. *J. China Univ. Pet., Ed. Nat. Sci.* **2011**, *35* (5), 6−13.

(40) Taylor, K. G.; Gawthorpe, R. L.; Curtis, C. D.; Marshall, J. D.; Awwiller, D. N. Carbonate cementation in a sequence-stratigraphic framework: Upper Cretaceous sandstones, Book Cliffs, Utah-Colorado. *J. Sediment. Res.* **2000**, *70* (2), 360−372.

(41) Wu, S. *Carbonate Cements and Their Formation Mechanism in Palaeogene Sandstones of Lishui Sag*; Chengdu University of Technology: Chengdu, 2006; pp 31−35.

(42) Meshri, I. D. On the reactivity of carbonic and organic acids and generation of secondary porosity. *SEPM Spec. Publ.* **1986**, *38*, 123−128.

(43) Friedman, I.; O'Neil, J. R. Compilation of Stable Isotope Fractionation Factors of Geochemical Interest. In *Data of Geochemistry*; US Government Printing Office, 1997; pp 1−4.

(44) Shackleton, N.; Kennett, J. Paleotemperature History of the Cenozoic and the Initiation of Antarctic Glaciation: Oxygen and Carbon Isotope Analyses in DSDP Sites 277, 279, and 281. In *Ligament Balancing*; Springer-Verlag: Berlin and Heidelberg, 1976; pp 3−6.

(45) Wang, D. *The Carbonate Cements and Its Formation Mechanism and Distribution Characteristics in the Deep Reservoir Sandstone in Baiyun Sag*; Northwest University: Xi'an, 2016; pp 31−38.

(46) Keith, M. L.; Weber, J. N. Carbon and oxygen isotopic composition of selected limestones and fossils. *Geochim. Cosmochim. Acta* **1964**, *28* (10−11), 1787−1816.

(47) Huang, W. *Hydrocarbon Generation Kinetics and Geochemical Characteristics of Coaly Source Rocks in the Kuqa Depression*; Guangzhou Institute of Geochemistry, Chinese Academy of Sciences, 2019; pp 78−93.

(48) Yang, H.; Gong, W.; Zheng, L. Characteristics of oil and gas generation, expelling and retention of coaly source rock. *Pet. Geol. Exp.* **2021**, *43* (3), 498−506.

(49) Liu, N. *Study on Fluids Transportation and Water-rock Interactions of CO_2 Geological Storage in Sandstone Reservoirs in Continental Sedimentary Basins*; China University of Geosciences, 2018; pp 67−82.

(50) Huang, K.; Huang, S.; Tong, H.; Liu, L. Thermodynamic calculation of feldspar dissolution and its significance on research of clastic reservoir. *Geol. Bull. China* **2009**, *28* (4), 474−482.